

SLfRank: Shinnar-Le-Roux Pulse Design with Reduced Energy and Accurate Phase Profiles using Rank Factorization

Frank Ong, Michael Lustig, Shreyas Vasanawala, and John Pauly

Abstract—The Shinnar-Le-Roux (SLR) algorithm is widely used to design frequency selective pulses with large flip angles. We improve its design process to generate pulses with lower energy (by as much as 26%) and more accurate phase profiles.

Concretely, the SLR algorithm consists of two steps: (1) an invertible transform between frequency selective pulses and polynomial pairs that represent Cayley-Klein (CK) parameters and (2) the design of the CK polynomial pair to match the desired magnetization profiles. Because the CK polynomial pair is bi-linearly coupled, the original algorithm sequentially solves for each polynomial instead of jointly. This results in sub-optimal pulses.

Instead, we leverage a convex relaxation technique, commonly used for low rank matrix recovery, to address the bi-linearity. Our numerical experiments show that the resulting pulses are almost always globally optimal in practice. For slice excitation, the proposed algorithm results in more accurate linear phase profiles. And in general the improved pulses have lower energy than the original SLR pulses.

Index Terms—MRI, RF Pulse Design, Shinnar-Le-Roux Algorithm, Convex Relaxation, Low Rank Matrix

I. INTRODUCTION

Frequency selective radio-frequency (RF) pulses are essential components in magnetic resonance imaging (MRI). Among other functions, they are used for slice excitation, spectral saturation, and spin-echo refocusing. Several accelerated imaging techniques, such as simultaneous multi-slice imaging, further build on advances in RF pulse design. Improvements in frequency selective pulse design can therefore benefit many applications.

The Shinnar-Le-Roux (SLR) algorithm [1]–[9] is widely used to design frequency selective pulses with large flip angles. It vastly simplifies the highly non-linear pulse design problem by mapping RF pulses to pairs of polynomial that represent Cayley-Klein (CK) parameters. Pulse designers can then solve for polynomial pairs using filter design algorithms and convert them back. Users can also incorporate pulse energy as a design objective, which is crucial when the specific absorption rate (SAR) is a limiting factor.

However, there is a subtle issue in the current SLR design process: the algorithm does not jointly design the CK polynomial pair. This can lead to sub-optimal pulses with higher energy and inaccurate phase profiles.

The main challenge preventing joint recovery is that CK parameters are bi-linearly coupled. For example, the transverse

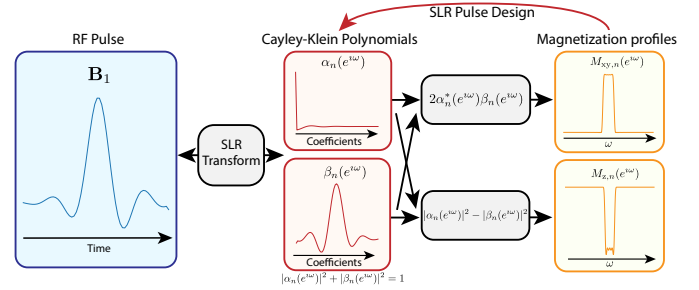


Fig. 1: An overview of the SLR algorithm, which consists of two steps: (1) an invertible transform between frequency selective pulses and polynomial pairs that represent Cayley-Klein (CK) parameters and (2) the design of the CK polynomial pair to match a desired magnetization profile. Because the CK polynomial pair is bi-linearly coupled, the original algorithm sequentially solves for each polynomial instead of jointly. This results in sub-optimal pulses. Instead, we propose an improved SLR (SLfRank) design process that can jointly solve for the CK polynomial pair. The new design can specify constraints directly on magnetization profiles, and optimize both CK polynomials to minimize pulse energy. In particular, we leverage a convex relaxation technique, commonly used for low rank matrix recovery, to address the bi-linearity.

magnetization M_{xy} is related to the CK parameters, α and β , as $M_{xy} = 2\alpha^*\beta$. To bypass the bi-linear coupling, the SLR algorithm first converts constraints on M_{xy} to constraints on β . It then finds a β to satisfy the constraints, and solves for an α to minimize pulse energy. The conversion between constraints on magnetization profiles and on β is not exact. SLR pulses can produce different phase profiles than the desired ones because the design does not account for the phase of α . Such process also does not recover the β that minimizes energy.

To correct for phase profile errors in the SLR algorithm, Barral et al. [10] proposed a heuristic to alternatively solve for CK parameters. While effective, the method does not jointly optimize the CK polynomials to minimize pulse energy. Besides the SLR algorithm, other pulse design methods present different tradeoffs. A line of work using the inverse scattering transform [11]–[17] can specify constraints on magnetization profiles and minimize pulse energy. But the resulting pulses have infinite lengths. Optimal control methods [18] have also been extensively used for pulse design. However, it is not clear in practice whether the resulting pulses achieve minimal energy.

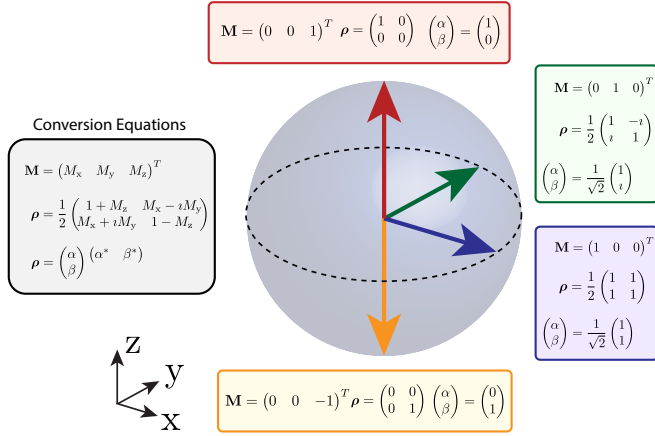


Fig. 2: Illustration of different representations: magnetization vector \mathbf{M} , quaternion ρ , and Cayley-Klein (CK) parameters α and β . We can map vectors to quaternions using an orthogonal matrix basis formed by the Pauli matrices and the identity matrix. CK parameters are simply rank-one factors of quaternions. This shows the bi-linear relationship between magnetization vectors and CK parameters.

We propose an improved SLR design process to jointly solve for the CK polynomial pair. The new design can specify constraints directly on magnetization profiles, and optimize both CK polynomials to minimize pulse energy. In particular, we leverage a convex relaxation technique, commonly used for low rank matrix recovery, to address the bi-linearity. Although we relax the problem, the convex program allows us to check for optimality. And our numerical experiments show that the resulting pulses almost always attain the global solution in practice. Because the algorithm is based on rank factorization, we name the proposed algorithm SLfRank.

Following [9], we use SLfRank to design pulses for excitation, inversion, saturation, and spin-echo refocusing. For slice excitation, the pulses result in more accurate linear phase profiles. And in general they have lower energy than the original SLR pulses by as much as 26%.

II. OVERVIEW OF THE SLR ALGORITHM

Here we give an overview of the original SLR algorithm, which consists of two steps: (1) an invertible transform between frequency selective pulses and polynomial pairs that represent CK parameters and (2) the design of the CK polynomial pair to match a desired magnetization profile.

Our work only improves the design aspect. But we describe the transform as well for completeness. We also highlight its use of quaternion representations, which provides insight to the proposed convex program.

We assume our readers are familiar with the classical Bloch equation in vector representation, but not necessarily in other forms. Therefore, we first give an introduction to the different representations used in the SLR algorithm.

A. Vectors to Quaternions to Cayley-Klein Parameters

We begin by going over the relationship between magnetization vectors and CK parameters. We use the quaternion as an intermediate representation, which allows us to map

vectors to quaternions, and then to CK parameters. This path exposes the bi-linear relationship between vectors and CK parameters, which we focus on in later sections. Figure 2 provides illustrative examples of different representations.

Concretely, let us define the following matrices:

$$\mathbf{I} = \begin{pmatrix} 1 & 0 \\ 0 & 1 \end{pmatrix} \quad \sigma_x = \begin{pmatrix} 0 & 1 \\ 1 & 0 \end{pmatrix}$$

$$\sigma_y = \begin{pmatrix} 0 & -i \\ i & 0 \end{pmatrix} \quad \sigma_z = \begin{pmatrix} 1 & 0 \\ 0 & -1 \end{pmatrix}$$

where $i = \sqrt{-1}$. The matrices σ_x , σ_y , and σ_z are often called the Pauli matrices. Together with the identity matrix \mathbf{I} , they form an orthogonal basis for 2-by-2 Hermitian matrices.

Then, for any magnetization vector $\mathbf{M} = (M_x \ M_y \ M_z)^T$, we can convert it to a quaternion ρ as

$$\rho = \frac{1}{2} (\mathbf{I} + M_x \sigma_x + M_y \sigma_y + M_z \sigma_z) \quad (1)$$

$$= \frac{1}{2} \begin{pmatrix} 1 + M_z & M_x - iM_y \\ M_x + iM_y & 1 - M_z \end{pmatrix}. \quad (2)$$

Note that the trace of ρ is one by construction.

Quaternions can be seen as extensions of complex numbers, with the Pauli matrices acting like the imaginary number. And just as complex numbers can easily represent two-dimensional rotations, quaternions can compactly describe three-dimensional rotations.

In particular, if we want to rotate a quaternion ρ around a unit-norm axis $\mathbf{u} = (u_x \ u_y \ u_z)^T$ by angle θ , then defining $\mathbf{u} \cdot \boldsymbol{\sigma} = u_x \sigma_x + u_y \sigma_y + u_z \sigma_z$, the rotated quaternion $\mathcal{R}_{\theta\mathbf{u}}(\rho)$ can be expressed as

$$\mathcal{R}_{\theta\mathbf{u}}(\rho) = e^{i\theta(\mathbf{u} \cdot \boldsymbol{\sigma})/2} \rho e^{-i\theta(\mathbf{u} \cdot \boldsymbol{\sigma})/2}, \quad (3)$$

where the exponential is a matrix exponential given by

$$e^{i\theta(\mathbf{u} \cdot \boldsymbol{\sigma})/2} = \mathbf{I} \cos(\theta/2) + i(\mathbf{u} \cdot \boldsymbol{\sigma}) \sin(\theta/2).$$

This simple rotation representation makes quaternions ideal for describing spin dynamics.

Another useful property of quaternions is that the rank of a quaternion is related to the norm of the equivalent magnetization vector. A quaternion ρ is always positive semi-definite as long as its vector representation \mathbf{M} has norm less than one. That is,

$$\rho \succeq 0 \Leftrightarrow |M_x|^2 + |M_y|^2 + |M_z|^2 \leq 1.$$

This can be seen from the Schur complement of ρ , $[1 - M_z - |M_{xy}|^2/(1 + M_z)]/2$, which is non-negative if and only if ρ is positive semi-definite.

Moreover, if the vector representation has unit norm, then the Schur complement is zero. This implies that the quaternion is rank deficient. Because the trace of the quaternion is one by construction, the rank can only be one. Therefore, we obtain

$$\rho = \begin{pmatrix} \alpha \\ \beta \end{pmatrix} \begin{pmatrix} \alpha^* & \beta^* \end{pmatrix} \Leftrightarrow |M_x|^2 + |M_y|^2 + |M_z|^2 = 1, \quad (4)$$

for some $\alpha \in \mathbb{C}$ and $\beta \in \mathbb{C}$ such that $|\alpha|^2 + |\beta|^2 = 1$.

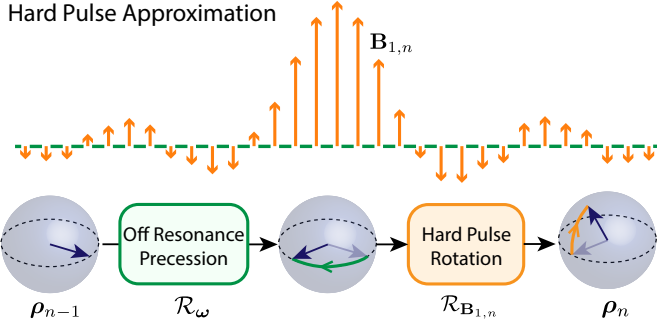


Fig. 3: The SLR algorithm considers the hard pulse approximation, which discretizes the RF pulse to a sequence of impulses, also known as hard pulses. The magnetization evolution can then be described as a recursion of off resonance precession followed by hard pulse rotation. Off resonance rotates magnetization around the z-axis. And a hard pulse rotates magnetization around an axis in the transverse plane.

The parameters α and β are often called the Cayley-Klein (CK) parameters. Because rotation operators in Eq. (3) preserve the quaternion rank, CK parameters can always represent magnetization in the absence of relaxation effects. Note also that the energy of CK parameters must sum to one. That is,

$$\alpha\alpha^* + \beta\beta^* = 1.$$

To convert between CK parameters and magnetization vectors, we simply match equations (2) and (4), and obtain

$$M_{xy} = 2\beta\alpha^* \text{ and } M_z = \alpha\alpha^* - \beta\beta^*,$$

which explicitly shows the bi-linear relationship between CK parameters and magnetization vectors.

In summary, we can convert vectors to quaternions using the Pauli matrices. CK parameters are then factors of quaternions when energy is conserved.

B. Forward SLR Transform

With the quaternion and CK parameter representations, we can obtain the forward SLR transform by going through a discretized version of the Bloch equation. In particular, the forward SLR transform converts any RF pulse to two polynomials that represent CK parameters.

To do so, the forward SLR transform first considers the hard pulse approximation, which discretizes the RF pulse to a sequence of impulses, also known as hard pulses. The magnetization evolution then becomes a recursion of off resonance precession followed by hard pulse rotation. Off resonance rotates magnetization around the z-axis. And a hard pulse rotates magnetization around an axis in the transverse plane. Figure 3 provides an illustration.

Concretely, let $\omega = (0 \ 0 \ \omega)^T$ represent off-resonance with frequency ω in radian and $\mathbf{B}_{1,n} = (B_{1,x,n} \ B_{1,y,n} \ 0)^T$ represent the n th hard pulse in radian, then the quaternion after the n th hard pulse is given by

$$\rho_n = \mathcal{R}_{\mathbf{B}_{1,n}}(\mathcal{R}_\omega(\rho_{n-1})). \quad (5)$$

Using equation (3), we obtain the following expressions for the rotation operators:

$$\mathcal{R}_{\mathbf{B}_{1,n}}(\rho) = \begin{pmatrix} c_n & -s_n^* \\ s_n & c_n \end{pmatrix} \rho \begin{pmatrix} c_n & s_n^* \\ -s_n & c_n \end{pmatrix}$$

$$\mathcal{R}_\omega(\rho) = \begin{pmatrix} 1 & 0 \\ 0 & z^{-1} \end{pmatrix} \rho \begin{pmatrix} 1 & 0 \\ 0 & z \end{pmatrix}$$

where

$$\begin{aligned} c_n &= \cos(\|\mathbf{B}_{1,n}\|/2), \\ s_n &= \frac{i(B_{1,x,n} + iB_{1,y,n})}{\|\mathbf{B}_{1,n}\|} \sin(\|\mathbf{B}_{1,n}\|/2), \\ z &= e^{i\omega}. \end{aligned}$$

We can further simplify the forward evolution by using CK parameters as representations. Substituting the rotation operators and using equation (4), we have

$$\begin{pmatrix} \alpha_n \\ \beta_n \end{pmatrix} = \begin{pmatrix} c_n & -s_n^* \\ s_n & c_n \end{pmatrix} \begin{pmatrix} 1 & 0 \\ 0 & z^{-1} \end{pmatrix} \begin{pmatrix} \alpha_{n-1} \\ \beta_{n-1} \end{pmatrix}. \quad (6)$$

In each time step, the CK parameters gain one additional z factor. Therefore, starting from an initial CK parameter $\alpha_0 = 1$ and $\beta_0 = 0$ at equilibrium, the CK parameters after the n th hard pulse become degree- $(n-1)$ polynomials in z . That is

$$\begin{aligned} \alpha_n(z) &= \sum_{j=0}^{n-1} a_{n,i} z^{-j}, \\ \beta_n(z) &= \sum_{j=0}^{n-1} b_{n,i} z^{-j}. \end{aligned} \quad (7)$$

Note that the energy of the CK parameters is preserved for all n . That is,

$$\alpha_n(z)\alpha_n^*(z) + \beta_n(z)\beta_n^*(z) = 1. \quad (8)$$

And we can easily obtain magnetization vectors after the n th hard pulse as:

$$\begin{aligned} M_{xy,n}(z) &= 2\beta_n(z)\alpha_n^*(z) \\ M_{z,n}(z) &= \alpha_n(z)\alpha_n^*(z) - \beta_n(z)\beta_n^*(z), \end{aligned} \quad (9)$$

In summary, under the hard pulse approximation, the forward SLR transform can convert any RF pulse to two polynomials that represent the CK parameters, as shown in Eq. (7). The polynomials must also satisfy an energy constraint in Eq. (8). What is remarkable is that given two polynomials with the energy constraint, we can always convert them back to a valid pulse with the inverse SLR transform.

C. Inverse SLR Transform

Given any polynomial pair that satisfy the energy constraint in Eq. (8), the inverse SLR transform can map it back to an RF pulse. It does so by considering the following backward recursion of Eq. (6):

$$\begin{pmatrix} \alpha_{n-1} \\ \beta_{n-1} \end{pmatrix} = \begin{pmatrix} 1 & 0 \\ 0 & z \end{pmatrix} \begin{pmatrix} c_n & s_n^* \\ -s_n & c_n \end{pmatrix} \begin{pmatrix} \alpha_n \\ \beta_n \end{pmatrix}.$$

It then recovers c_n and s_n such that α_{n-1} and β_{n-1} represent valid CK parameters.

For α_{n-1} and β_{n-1} to be valid, they need to be degree- $(n-2)$ polynomials and satisfy the energy constraint. Note that as long as $|c_n|^2 + |s_n|^2 = 1$, the energy constraint is satisfied. To ensure α_{n-1} and β_{n-1} are degree- $(n-2)$ polynomials, we need

$$-s_n a_{n,0} + c_n b_{n,0} = 0 \quad (10)$$

$$c_n a_{n,n-1} + s_n^* b_{n,n-1} = 0, \quad (11)$$

which allow us to solve for two sets of solutions for c_n and s_n .

It turns out these two solutions are the same because the energy constraint in Eq. (8) implies

$$a_{n,n-1} a_{n,0}^* + b_{n,n-1} b_{n,0}^* = 0,$$

where the left hand side is the leading coefficient of the polynomial $\alpha_n(z)\alpha_n^*(z) + \beta_n(z)\beta_n^*(z)$.

Therefore, we can recover the parameters as:

$$c_n = \frac{a_{n,0}}{\sqrt{|a_{n,0}|^2 + |b_{n,0}|^2}} = \frac{b_{n,n-1}}{\sqrt{|a_{n,n-1}|^2 + |b_{n,n-1}|^2}}$$

$$s_n = \frac{b_{n,0}}{\sqrt{|a_{n,0}|^2 + |b_{n,0}|^2}} = \frac{-a_{n,n-1}^*}{\sqrt{|a_{n,n-1}|^2 + |b_{n,n-1}|^2}}$$

And we can obtain the n th hard pulse as,

$$\|\mathbf{B}_{1,n}\|_2 = 2 \arctan\left(\left|\frac{s_n}{c_n}\right|\right),$$

$$B_{1,n,x} = \|\mathbf{B}_{1,n}\|_2 \frac{1 - \text{Im}(s_n)^2}{|c_n|^2},$$

$$B_{1,n,y} = \|\mathbf{B}_{1,n}\|_2 \frac{1 - \text{Re}(s_n)^2}{|c_n|^2}.$$

D. Original SLR Design Process

With the SLR transform, the highly non-linear pulse design problem becomes equivalent to designing the CK polynomial pair. The remaining challenge is the bi-linear coupling between α_n and β_n . The original SLR algorithm bypasses this by sequentially solving for each variable. It first converts design constraints on magnetization profiles to constraints on β_n . Then, it recovers an α_n that minimizes the pulse energy. In the following, we highlight some advantages and disadvantages of this approach.

There are certain constraints that can be directly expressed in β_n . [9] shows that for spin-echo refocusing pulses, the effective transverse magnetization after crusher gradients can be expressed as

$$M_{xy,n}(z) = \beta_n^2(z).$$

For single band designs, any constraints on $M_{xy,n}$ can then be converted to constraints on β_n up to a global sign change, which does not affect the resulting pulse.

However, for other pulses, we cannot directly translate constraints. Instead, using Eqs. (8) and (9), we only have the following relationships:

$$|M_{xy,n}(z)|^2 = 4|\beta_n(z)|^2(1 - |\beta_n(z)|^2),$$

$$M_{z,n}(z) = 1 - 2|\beta_n(z)|^2.$$

[9] shows that we can use these equations to specify ripple parameters in min-max filter designs. However, note that we cannot express transverse magnetization phase in terms of β_n .

When the user does not require a particular transverse magnetization phase profile, the original SLR algorithm has more flexibility. One choice is a minimum phase polynomial for β_n . This is equivalent to selecting a β_n polynomial that maximizes its first coefficient $\text{Re}\{b_{n,0}\}$. Using linear approximation, we can interpret this as maximizing the last hard pulse:

$$\text{Re}\{b_{n,0}\} = c_1 \dots c_{n-1} s_n \approx B_{1,y,n}/2.$$

However, when the user wants a specific transverse magnetization phase response, such as in slice excitation, the original SLR algorithm cannot find a corresponding β_n polynomial to do so. Instead, it relies on an approximation that α_n does not contribute much phase and finds a β_n to account for all of the phase of M_{xy} . But α_n always contributes some phase. Therefore, the resulting profile in general deviates from the desired one.

Once we obtain a β_n , the original design process recovers the α_n polynomial by minimizing pulse energy. In particular, the first polynomial coefficient of α_n acts as a proxy for pulse energy. Using $c_j \approx 1 - \|\mathbf{B}_{1,j}\|^2/8$, we have

$$a_{n,0} = c_1 c_2 \dots c_n \approx 1 - \frac{1}{8} \sum_{j=1}^n \|\mathbf{B}_{1,j}\|^2.$$

With fine enough discretization, maximizing $a_{n,0}$ minimizes pulse energy. We can then find the corresponding α_n by solving for a minimum phase filter.

On the other hand, the β_n polynomial design does not take pulse energy into consideration. It is possible a different β_n that satisfy the constraints results in lower pulse energy. Indeed, our improved SLR design shows that jointly designing α_n and β_n reduces pulse energy in general.

III. SLFRANK: IMPROVED SLR PULSE DESIGN WITH RANK FACTORIZATION

We propose an improved SLR design, named SLFRank, to jointly recover the CK polynomials with a convex program. The new design can specify constraints directly on magnetization profiles, and optimize both CK polynomials to minimize pulse energy. To derive the optimization problem, we first show that all constraints on the CK polynomials can be represented as linear equations on a rank-one matrix. Then we relax matrix rank constraints to positive semi-definite matrix constraints to obtain a convex program.

Concretely let us define the following vectors:

$$\boldsymbol{\psi}(z) = (1 \quad z \quad \dots \quad z^{n-1})^T$$

$$\mathbf{a} = (a_{n,0} \quad a_{n,1} \quad \dots \quad a_{n,n-1})^T$$

$$\mathbf{b} = (b_{n,0} \quad b_{n,1} \quad \dots \quad b_{n,n-1})^T$$

Then the CK polynomials can be expressed as,

$$\alpha_n(z) = \boldsymbol{\psi}^*(z)\mathbf{a},$$

$$\beta_n(z) = \boldsymbol{\psi}^*(z)\mathbf{b}.$$

Let us further define \mathbf{P} as the outer product of the CK polynomial coefficients:

$$\mathbf{P} = \begin{pmatrix} \mathbf{P}_{aa} & \mathbf{P}_{ab} \\ \mathbf{P}_{ba} & \mathbf{P}_{bb} \end{pmatrix} = \begin{pmatrix} \mathbf{a} \\ \mathbf{b} \end{pmatrix} \begin{pmatrix} \mathbf{a}^* & \mathbf{b}^* \end{pmatrix}$$

Then, we can express the energy constraint in Eq. (8) and magnetization profiles in terms of \mathbf{P} as follows:

$$\begin{aligned} 1 &= \psi^*(z)(\mathbf{P}_{aa} + \mathbf{P}_{bb})\psi(z) \\ M_{xy,n}(z) &= 2\psi^*(z)\mathbf{P}_{ba}\psi(z) \\ M_{z,n}(z) &= \psi^*(z)(\mathbf{P}_{aa} - \mathbf{P}_{bb})\psi(z). \end{aligned}$$

The above equations show that we can express all constraints on the CK polynomials as linear equations on a rank-one matrix \mathbf{P} . We can also easily change them to impose inequality constraints on magnetization profiles.

Taking a step back, the matrix \mathbf{P} we have just formed effectively represents the underlying quaternion $\rho_n(z)$. In particular, we have

$$\rho_n(z) = \begin{pmatrix} \psi^*(z) & \mathbf{0} \\ \mathbf{0} & \psi^*(z) \end{pmatrix} \mathbf{P} \begin{pmatrix} \psi(z) & \mathbf{0} \\ \mathbf{0} & \psi(z) \end{pmatrix}$$

Therefore, one way to interpret the proposed design is that we solve for quaternions instead of CK parameters. And the two representations become equivalent when the quaternion is rank-one.

Optimizing over rank-one matrices is in general non-convex. A common strategy is to relax the rank constraint into a positive semi-definite matrix constraint. Concretely, we can relax the constraint as follows,

$$\mathbf{P} \succeq \begin{pmatrix} \mathbf{a} \\ \mathbf{b} \end{pmatrix} \begin{pmatrix} \mathbf{a}^* & \mathbf{b}^* \end{pmatrix}.$$

Similar to the original SLR algorithm, we maximize $a_{n,0}$ to minimize pulse energy and $b_{n,0}$ to generate minimum phase pulses. Putting everything together, we obtain the following optimization problem to design the CK polynomials:

$$\begin{aligned} \max \quad & \text{Re}(a_{n,0}) + \lambda_{\text{mp}} \text{Re}(b_{n,0}) \\ \text{s.t.} \quad & \mathbf{P} \succeq \begin{pmatrix} \mathbf{a} \\ \mathbf{b} \end{pmatrix} \begin{pmatrix} \mathbf{a}^* & \mathbf{b}^* \end{pmatrix}, \\ & \psi^*(e^{i\omega})(\mathbf{P}_{aa} + \mathbf{P}_{bb})\psi(e^{i\omega}) = 1, \\ & |2\psi^*(e^{i\omega})\mathbf{P}_{ba}\psi(e^{i\omega}) - M_{xy,n}(e^{i\omega})| \leq \delta_{xy}(e^{i\omega}), \\ & |\psi^*(e^{i\omega})(\mathbf{P}_{aa} - \mathbf{P}_{bb})\psi(e^{i\omega}) - M_{z,n}(e^{i\omega})| \leq \delta_z(e^{i\omega}), \\ & |\psi^*(e^{i\omega})\mathbf{b} - \beta_n(e^{i\omega})| \leq \delta_\beta(e^{i\omega}), \end{aligned}$$

where ω goes from $-\pi$ to π , λ_{mp} enforces minimum phase conditions, and δ_{xy} , δ_z , and δ_β are user-defined error parameters.

Although we relax the problem, the convex program allows us to check for optimality with the solution rank. If the resulting matrix \mathbf{P} is close to rank-one, then it is close to being globally optimal. And if it is exactly rank-one, then we have recovered a global minimum. In the next section, our numerical experiments will show that convex program almost always attains the global solution in practice.

Finally, the convex program in its current form imposes infinitely many constraints due to the continuous nature of ω .

There are two ways to address this. One way is to finely sample frequencies and only impose constraints on the finite set. We opt for this strategy for the inequalities because it is simpler. And slight violation outside the finite set is often tolerable in practice. Another way is to convert the constraints into linear equations on positive semi-definite matrices as shown in [19]. In particular, the constraint $\psi^*(e^{i\omega})(\mathbf{P}_{aa} + \mathbf{P}_{bb})\psi(e^{i\omega}) = 1$ for all ω is equivalent to

$$\sum_{i,j:i-j=k} (\mathbf{P}_{aa} + \mathbf{P}_{bb})_{ij} = \begin{cases} 1, & \text{if } k = 0 \\ 0, & \text{otherwise.} \end{cases}$$

for $k = -n, -n+1, \dots, n$. This ensures the resulting solution exactly satisfies the energy constraint.

IV. NUMERICAL EXPERIMENTS

We use the proposed algorithm to design pulses for excitation, inversion, saturation, and spin-echo refocusing. All examples shown here have time-bandwidths of 8, maximum absolute errors of 1%, and $n = 64$. The inequality constraints are imposed on 960 uniformly sampled points in the frequency domain. Table I and II contain the δ parameters used for different pulse types. For bands that are not specified, the δ parameters are set to 1 and the desired profiles are set to 0. For minimum phase pulses, λ_{mp} is set to one. Maximum phase pulses are generated as time-reversed minimum phase pulses. For all other pulses, λ_{mp} is set to zero.

Because the optimization problem is convex, any solver can reach a global minimum. We first verify the program with CVXPY [20], which uses interior-point solvers, with $n = 16$. While CVXPY is accurate, it can be quite slow for large n . For the final pulses displayed in this manuscript, we use the primal dual hybrid gradient algorithm [21] in SigPy [22] with $n = 64$. We use 20000 iterations to ensure the algorithm converges. We compare SLfRank pulses to the original SLR pulses generated with SigPy.RF [23]. We compute the pulse energy, defined as the sum of squares of the pulses, and peak amplitude for comparison.

In the spirit of reproducible research, we provide a software package to reproduce the results described in this paper. The software package can be downloaded from:

<https://github.com/MRSRL/slfrank>

Figures 4, 5, 6, 7, and 8 show the resulting pulses and their magnetization profiles. In all cases except for the minimum phase excitation pulse, the convex relaxation is tight, that is the resulting solution \mathbf{P} has rank one and

$$\mathbf{P} = \begin{pmatrix} \mathbf{a} \\ \mathbf{b} \end{pmatrix} \begin{pmatrix} \mathbf{a}^* & \mathbf{b}^* \end{pmatrix}.$$

For the minimum phase excitation pulse, the relaxation is still quite accurate with a 0.004 ℓ_2 norm difference between \mathbf{P} and the outer product of \mathbf{a} and \mathbf{b} .

Figure 4 shows the linear phase excitation pulses and their magnetization profiles after refocusing. The SLfRank pulse has a much flatter phase response after refocusing than the SLR pulse. Pulse energy is reduced from 0.318 to 0.259 (18.6%) and peak is reduced from 0.208 to 0.189 (9.1%). Note that

Pulse (phase)	Pass-band with ripple δ_1				Stop-band with ripple δ_2			
	M_{xy}	δ_{xy}	M_z	δ_z	M_{xy}	δ_{xy}	M_z	δ_z
Excitation (linear)	$e^{-i\omega(n+1)/2}$	δ_1	0	$\sqrt{1 - (1 - \delta_1)^2}$	0	δ_2	1	$1 - \sqrt{1 - \delta_2^2}$
Excitation (min.)	0	1	0	$\sqrt{1 - (1 - \delta_1)^2}$	0	δ_2	1	$1 - \sqrt{1 - \delta_2^2}$
Inversion (min.)	0	$\sqrt{1 - (1 - \delta_1)^2}$	-1	δ_1	0	$\sqrt{1 - (1 - \delta_2)^2}$	1	δ_2
Saturation (max.)	0	1	0	δ_1	0	1	1	δ_2

TABLE I: Parameters for excitation, inversion and saturation pulse designs.

Pulse (phase)	Pass-band with ripple δ_1		Stop-band with ripple δ_2	
	β	δ_β	β	δ_β
Spin-Echo (zero)	$-e^{-i\omega(n+1)/2}$	$(1 - \sqrt{1 - \delta_1})/2$	0	$\sqrt{\delta_2}$

TABLE II: Parameters for spin-echo refocusing pulse designs.

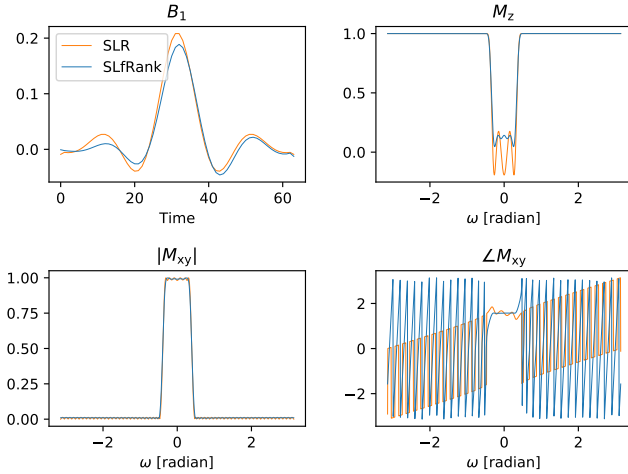


Fig. 4: Linear phase excitation pulses and their magnetization profiles after refocusing. The SLfRank pulse has a much flatter phase response than the original one after refocusing. Pulse energy is reduced from 0.318 to 0.259 (18.6%) and peak is reduced from 0.208 to 0.189 (9.1%). Note that the SLfRank pulse is asymmetric, whereas the SLR pulse is symmetric. This shows that the proposed design compensates for the phase of α to generate a linear phase profile.

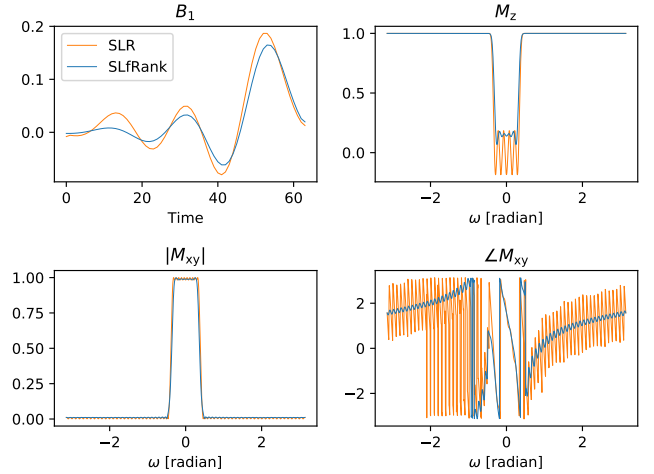


Fig. 5: Minimum phase slice selection pulses and their magnetization profiles. Pulse energy is reduced from 0.318 to 0.234 (26.4%) and peak is reduced from 0.187 to 0.165 (11.8%).

the SLfRank pulse is asymmetric, whereas the SLR pulse is symmetric. This shows that the proposed design compensates for the phase of α to generate a linear phase profile.

Figure 5 shows the minimum phase excitation pulses and their magnetization profiles. Pulse energy is reduced from 0.318 to 0.234 (26.4%) and peak is reduced from 0.187 to 0.165 (11.8%).

Figure 6 shows the maximum phase saturation pulses and their magnetization profiles. Pulse energy is reduced from 0.352 to 0.333 (5.40%) and peak is reduced from 0.212 to 0.208 (1.89%). The SLfRank pulse also has fewer discontinuities at the end of the pulse, commonly known as Connolly wings, when compared to the SLR pulse.

Figure 7 shows the minimum phase inversion pulses and their magnetization profiles. Pulse energy is reduced from 3.00 to 2.31 (23.0%) and peak is reduced from 0.781 to 0.679 (13.1%).

Finally, figure 8 shows the spin-echo refocusing pulses and their magnetization profiles. Pulse energy is reduced from 2.74 to 2.23 (18.6%) and peak is reduced from 0.827 to 0.716 (13.4%). The SLfRank pulse also has fewer discontinuities

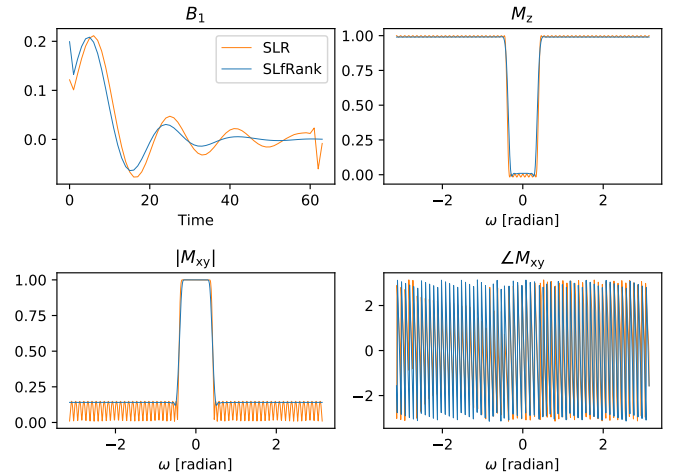


Fig. 6: Maximum phase saturation pulses and their magnetization profiles. Pulse energy is reduced from 0.352 to 0.333 (5.40%) and peak is reduced from 0.212 to 0.208 (1.89%). The SLfRank pulse also has fewer discontinuities at the end of the pulse, commonly known as Connolly wings, when compared to the SLR pulse.

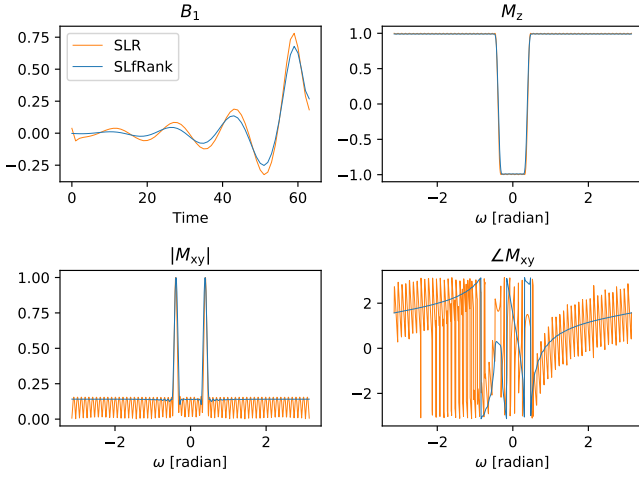


Fig. 7: Minimum phase inversion pulses and their magnetization profiles. Pulse energy is reduced from 3.00 to 2.31 (23.0%) and peak is reduced from 0.781 to 0.679 (13.1%).

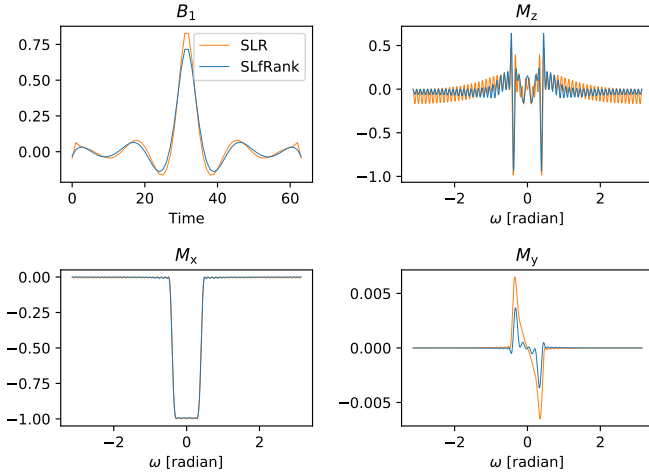


Fig. 8: Spin-echo refocusing pulses and their magnetization profiles. Pulse energy is reduced from 2.74 to 2.23 (18.6%) and peak is reduced from 0.827 to 0.716 (13.4%). The SLfRank pulse also has fewer discontinuities near the edges when compared to the SLR pulse.

near the edges when compared to the SLR pulse.

V. DISCUSSION

Our results show that joint optimization of CK polynomials can produce pulses with reduced energy and more accurate phase profiles. In our opinion, the reduced energy is the main feature of SLfRank pulses. Because SAR is proportional to pulse energy, SLfRank pulses can potentially accelerate acquisition time for SAR limited sequences. In addition, there is a slight reduction of peak pulse amplitude, which can be useful to prevent overflow in power amplifiers for simultaneous multi-slice imaging.

The accurate control over transverse magnetization phase in SLfRank allows us to obtain flatter phase response for slice excitation. However, this only provides marginal benefit in practice. As signals are contributed by summing across the

excited slice, variation in the slice profile does not affect the resulting signal-to-noise ratio much. The SLfRank algorithm can still be useful for other applications, where pulse designers want to design more exotic phase profiles.

For most examples in this manuscript, the proposed convex program can find a globally optimal solution. However, for the minimum phase excitation pulse design, there is still a slight gap between the solutions from the convex program and the rank-constrained problem. It is not clear to us whether this is a fundamental gap for such pulses. In particular, we observe that the convex program finds a rank-one solution when the ripple constraint is set to 2%. It is possible that there is a regime where the convex program produces globally optimal pulses.

Compared to the original SLR algorithm, SLfRank takes much longer to compute. On a workstation with two 16-core Intel Xeon Silver 4216 processors, the original SLR algorithm takes less than a second to run, whereas the SLfRank algorithm takes around two minutes. Because most pulse designs are not done online on scanners, we believe the running time of SLfRank is reasonable. But there are also several directions to improve its computation time, including leveraging the fast Fourier transform in the iterative algorithm and using GPUs.

Finally, one limitation of both the SLR and SLfRank algorithms is that they assume the initial magnetization starts from equilibrium except for the special case of spin-echo refocusing with crusher gradients. To generalize to arbitrary starting point, the SLR transform needs to be modified. And the design process should also be changed accordingly to form a complete SLR algorithm.

VI. CONCLUSION

We have shown an improved SLR design process that can jointly solve for the CK polynomial pair. The new design can specify constraints directly on magnetization profiles, and optimize both CK polynomials to minimize pulse energy. The pulses in general have lower energy and fewer discontinuities. They also have more accurate phase responses when compared to the original SLR pulses. With lower energy pulses, the SLfRank algorithm can potentially accelerate SAR-limited sequences. Moreover, it allows users to design arbitrary excitation phase profiles, which opens up new research opportunities.

REFERENCES

- [1] M. Shinnar and J. S. Leigh, "The application of spinors to pulse synthesis and analysis," *Magnetic Resonance in Medicine*, vol. 12, no. 1, pp. 93–98, Oct. 1989. [Online]. Available: <http://doi.wiley.com/10.1002/mrm.1910120112>
- [2] M. Shinnar, S. Eleff, H. Subramanian, and J. S. Leigh, "The synthesis of pulse sequences yielding arbitrary magnetization vectors," *Magnetic Resonance in Medicine*, vol. 12, no. 1, pp. 74–80, Oct. 1989. [Online]. Available: <http://doi.wiley.com/10.1002/mrm.1910120109>
- [3] M. Shinnar, L. Bolinger, and J. S. Leigh, "The synthesis of soft pulses with a specified frequency response," *Magnetic Resonance in Medicine*, vol. 12, no. 1, pp. 88–92, Oct. 1989. [Online]. Available: <http://doi.wiley.com/10.1002/mrm.1910120111>
- [4] —, "Use of finite impulse response filters in pulse design," in *Proceedings of the 7th Annual Meeting and Exhibition of the Society for Magnetic Resonance in Medicine*, San Francisco, CA, USA, 1988, p. 695. eprint: <https://onlinelibrary.wiley.com/doi/pdf/10.1002/mrm.22419880204>. [Online]. Available: <https://onlinelibrary.wiley.com/doi/abs/10.1002/mrm.22419880204>

- [5] —, “The use of finite impulse response filters in pulse design,” *Magnetic Resonance in Medicine*, vol. 12, no. 1, pp. 81–87, Oct. 1989. [Online]. Available: <http://doi.wiley.com/10.1002/mrm.1910120110>
- [6] P. Le Roux, “Exact Synthesis of Radiofrequency Waveforms,” in *Proceedings of the 7th Annual Meeting and Exhibition of the Society for Magnetic Resonance in Medicine*, San Francisco, CA, USA, Aug. 1988, p. 1049, eprint: <https://onlinelibrary.wiley.com/doi/pdf/10.1002/mrmp.22419880211>. [Online]. Available: <https://onlinelibrary.wiley.com/doi/abs/10.1002/mrmp.22419880211>
- [7] —, “Method of radio-frequency excitation in an NMR experiment,” US Patent US4940940A, Jul., 1990, library Catalog: Google Patents. [Online]. Available: <https://patents.google.com/patent/US4940940/en>
- [8] —, “Simplified RF Synthesis,” in *Proceedings of the 8th Annual Meeting and Exhibition of the Society for Magnetic Resonance in Medicine*, vol. 1989, Amsterdam, The Netherlands, Aug. 1989, p. 1168, eprint: <https://onlinelibrary.wiley.com/doi/pdf/10.1002/mrmp.22419890305>. [Online]. Available: <https://onlinelibrary.wiley.com/doi/abs/10.1002/mrmp.22419890305>
- [9] J. Pauly, P. L. Roux, D. Nishimura, and A. Macovski, “Parameter relations for the Shinnar-Le Roux selective excitation pulse design algorithm (NMR imaging),” *IEEE Transactions on Medical Imaging*, vol. 10, no. 1, pp. 53–65, Mar. 1991.
- [10] J. K. Barral, J. M. Pauly, and D. G. Nishimura, “SLR RF Pulse Design for Arbitrarily-Shaped Excitation Profiles,” in *Proceedings of the ISMRM 16th Annual Meeting*, Toronto, ON, Canada, May 2008, p. 1323.
- [11] C. L. Epstein, “Introduction to magnetic resonance imaging for mathematicians,” *Annales de l’institut Fourier*, vol. 54, no. 5, pp. 1697–1716, 2004. [Online]. Available: https://aif.centre-mersenne.org/item/AIF_2004__54_5_1697_0/
- [12] C. L. Epstein and J. F. Magland, “Inverse Scattering Pulse Design,” in *eMagRes*. American Cancer Society, 2012, eprint: <https://onlinelibrary.wiley.com/doi/pdf/10.1002/9780470034590.emrstml303>. [Online]. Available: <http://onlinelibrary.wiley.com/doi/abs/10.1002/9780470034590.emrstml303>
- [13] C. L. Epstein, “Minimum energy pulse synthesis via the inverse scattering transform,” *Journal of Magnetic Resonance*, vol. 167, no. 2, pp. 185–210, Apr. 2004. [Online]. Available: <https://linkinghub.elsevier.com/retrieve/pii/S1090780703004439>
- [14] —, “Minimum energy pulse synthesis via the inverse scattering transform,” *Journal of Magnetic Resonance*, vol. 167, no. 2, pp. 185–210, Apr. 2004. [Online]. Available: <http://linkinghub.elsevier.com/retrieve/pii/S1090780703004439>
- [15] J. F. Magland, “Discrete Inverse Scattering Theory for NMR Pulse Design,” *arXiv:0903.4363 [math-ph]*, Mar. 2009, arXiv: 0903.4363. [Online]. Available: <http://arxiv.org/abs/0903.4363>
- [16] J. Magland and C. L. Epstein, “Exact half pulse synthesis via the inverse scattering transform,” *Journal of Magnetic Resonance*, vol. 171, no. 2, pp. 305–313, Dec. 2004. [Online]. Available: <https://linkinghub.elsevier.com/retrieve/pii/S1090780704003040>
- [17] —, “Practical pulse synthesis via the discrete inverse scattering transform,” *Journal of Magnetic Resonance*, vol. 172, no. 1, pp. 63–78, Jan. 2005. [Online]. Available: <http://linkinghub.elsevier.com/retrieve/pii/S1090780704002800>
- [18] S. Conolly, D. Nishimura, and A. Macovski, “Optimal Control Solutions to the Magnetic Resonance Selective Excitation Problem,” *IEEE Transactions on Medical Imaging*, vol. 5, no. 2, pp. 106–115, Jun. 1986.
- [19] B. Dumitrescu, *Positive trigonometric polynomials and signal processing applications*, ser. Signals and communication technology. Dordrecht: Springer, 2007, oCLC: 85842464.
- [20] S. Diamond and S. Boyd, “CVXPY: a python-embedded modeling language for convex optimization,” *The Journal of Machine Learning Research*, vol. 17, no. 1, pp. 2909–2913, Jan. 2016.
- [21] A. Chambolle and T. Pock, “A First-Order Primal-Dual Algorithm for Convex Problems with Applications to Imaging,” *Journal of Mathematical Imaging and Vision*, vol. 40, no. 1, pp. 120–145, May 2011. [Online]. Available: <http://link.springer.com/10.1007/s10851-010-0251-1>
- [22] F. Ong and M. Lustig, “SigPy: A Python Package for High Performance Iterative Reconstruction,” in *Proceedings of the ISMRM 27th Annual Meeting*, Montreal, Quebec, Canada, May 2019, p. 4819. [Online]. Available: <https://cds.ismrm.org/protected/19MPresentations/abstracts/4819.html>
- [23] J. B. Martin, F. Ong, J. Ma, J. I. Tamir, M. Lustig, and W. A. Grissom, “SigPy.RF: Comprehensive Open-Source RF Pulse Design Tools for Reproducible Research,” in *Proceedings of the ISMRM 16th Annual Meeting*, Virtual, Aug. 2020, p. 1045.